



Inorganic–organic polymer electrolytes based on poly(vinyl alcohol) and borane/poly(ethylene glycol) monomethyl ether for Li-ion batteries

Hamide Aydın^a, Mehmet Şenel^a, Hamit Erdemi^b, Abdülhadi Baykal^a, Metin Tülü^a, Ali Ata^c, Ayhan Bozkurt^{a,*}

^a Department of Chemistry, Fatih University, 34500 Büyükdere-İstanbul, Turkey

^b Department of Polymer Engineering, Yalova University, 77100 Yalova, Turkey

^c Department of Materials Science and Engineering, Gebze Institute of Technology, 41400 Gebze-Kocaeli, Turkey

ARTICLE INFO

Article history:

Received 20 May 2010

Received in revised form 22 July 2010

Accepted 10 August 2010

Available online 17 August 2010

Keywords:

Poly(vinyl alcohol)

Poly(ethylene glycol) monomethyl ether (PEGME)

Borane–tetrahydrofuran

Polymer electrolytes

Li-ion conductivity

ABSTRACT

In this study, poly(vinyl alcohol) (PVA) was modified with poly(ethylene glycol) monomethyl ether (PEGME) using borane–tetrahydrofuran (BH₃/THF) complex. Molecular weights of both PVA and PEGME were varied prior to reaction. Boron containing comb-branched copolymers were produced and abbreviated as PVA1PEGMEX and PVA2PEGMEX. Then polymer electrolytes were successfully prepared by doping of the host matrix with CF₃SO₃Li at several stoichiometric ratios with respect to EO to Li. The materials were characterized via nuclear magnetic resonance (¹H NMR and ¹¹B NMR), Fourier transform infrared spectroscopy (FT-IR), Thermogravimetry (TG) and differential scanning calorimeter (DSC). The ionic conductivity of these novel polymer electrolytes were studied by dielectric-impedance spectroscopy. Li-ion conductivity of these polymer electrolytes depends on the length of the side units as well as the doping ratio. Such electrolytes possess satisfactory ambient temperature ionic conductivity (>10⁻⁴ S cm⁻¹). Cyclic voltammetry results illustrated that the electrochemical stability domain extends over 4V.

© 2010 Elsevier B.V. All rights reserved.

1. Introduction

Rechargeable lithium batteries have been investigated as an attractive alternative power source for a wide variety of applications. Lithium-based polymer electrolyte materials used in such battery systems, therefore, are considered an important research field [1–3]. It is expected that these materials should have high ionic conductivity, electrochemical stability and good mechanical properties for application [4]. Traditional polymer electrolytes containing a host polymer (such as poly[ethylene glycol], poly[ethylene oxide]) with lithium salts were found to exhibit relatively low conductivity, and introduction of small molecule plasticizers (such as propylene carbonate) to such polymer–salt systems was found to improve the conductivity of the materials [5,6]. In general, solid polymer electrolytes can be prepared by dissolving salt (LiX) in a suitable polymer matrix where there is an interaction between functional units of the host polymer and guest molecules [7–9]. In this context, polyethylene oxide (PEO) based electrolytes are the earliest and the most extensively studied systems [10,11].

The earliest works on the ionic conductivities of PEO complexed with alkali metal salts were made by Wright and Armand [12,13]. Depending on the salt concentration PEO based polymer electrolytes have semicrystalline morphology which may negatively affect the ionic conductivity especially at lower temperatures. In dry state these dry polymer electrolyte systems (PEO–LiX) offer lower ionic conductivity of the order of 10⁻⁶ S cm⁻¹ at ambient temperature.

In addition, gel polymer electrolytes can also be prepared by combination of a stable polymer matrix and special additives such as ethylene carbonate (EC), propylene carbonate (PC), dimethyl carbonate (DMC), *N*-methylpyrrolidinone (NMP) to promote ionic conductivity [14–16]. Polymers such as polyvinylidene fluoride (PVDF), polyacrylonitrile (PAN), poly(methyl methacrylate) (PMMA) and polyvinyl chloride (PVC) have been studied in polymer electrolytes [17–19]. These systems are comprised functional groups that are not sufficient to create charge separation between electrolyte ions. Thus, special additives are required to promote sufficient charge separation, which enable the ions in the solid matrix to respond to an electric field. In these systems, the major role of the polymer is mostly to maintain a solid and stable matrix, whereas the ion migration within the matrix under an electrical field is feasible because of the additives. However, the mechanical property of such polymer electrolytes is generally poor

* Corresponding author. Tel.: +90 212 8663300.

E-mail address: bozkurt@fatih.edu.tr (A. Bozkurt).

because of the characteristic of gels and additives [20]. Moreover, a variety of comb-branched polymers was investigated, in which PEO side chains were attached to a polymer backbone, which itself had a low glass transition temperature and thus giving rise to a more flexible system [1]. Polysiloxanes which include PEO side chains were studied by several groups [21–23]. These systems are liquids at RT and illustrated ionic conductivities of the around 10^{-4} S cm^{-1} after mixing with LiClO_4 . However, their chemical stabilities are poor due to the Si–O–C branched side chains.

Poly(vinyl alcohol) (PVA) is a water-soluble, polyhydroxy polymer whose physical properties are dependent on the degree of polymerization and degree of hydrolysis. PVA has an excellent chemical resistance; thus, it can be used in many practical applications such as adhesives, textile, and pharmaceutical and biomedical industries due to nontoxic and biodegradable properties [25–27]. PVA can also be modified by chemical cross-linking, which is a highly versatile method to improve the chemical, thermal, and mechanical properties [28]. One of the most common methods is the reaction of hydroxyl groups of PVA with aldehydes to form acetal or hemiacetal [29]. PVA can also physically cross-link with boric acid through hydrogen bonding and ionic interactions in the hydrated state [26,27]. PVA and a lithium salt, LiX, is the interesting membrane which may meet the requirements in terms of lithium conductivity and electrode compatibility.

In this work, PVA was modified with PEGME using BH_3/THF with different molecular weights of PVA and PEGME to produce boron containing comb-branched polymers. The attachment of PEGs to the polymer was investigated by FT-IR, ^1H NMR and ^{11}B NMR. Then polymer electrolytes were produced by doping with the $\text{CF}_3\text{SO}_3\text{Li}$ according to EO/Li ratio. The polymer electrolytes were characterized via FT-IR, TG and DSC. Li-ion conducting properties of the materials were investigated by dielectric-impedance analyzer and the results are discussed and compared with previously reported systems.

2. Experimental

2.1. Materials

PVA (degree of hydrolyzation $\geq 98\%$ $M_w = 72,000$ and $M_w = 145,000$) was provided from Merck, BH_3/THF (1.0 M solution in THF) and PEGME (average $M_n = 350, 550$ and 750) was purchased from Alfa Aesar Chemical Company. Dimethylsulfoxide (DMSO, analytical reagent) was obtained from Merck. $\text{CF}_3\text{SO}_3\text{Li}$ 97% was received from Alfa Aesar and stored in the glove box.

2.2. Polymer synthesis

The synthesis of the copolymers was carried out under the reflux, according to the esterification reaction shown in Fig. 1. In principle, the polymers were prepared by using BH_3/THF to link different PVAs and PEGMEs via the formation of boronate esters. PVAs with different molecular weights ($\text{PVA1} = 72,000$ and $\text{PVA2} = 145,000 \text{ g mol}^{-1}$) were used as main host matrix. PEGMEs with different molecular weights ($X = 350, 550$ and 750 g mol^{-1}) were used to introduce branches or side chain segments. The molar ratio between the reactants (BH_3 , PVA, PEGME) was kept at 1:1:2, respectively (for example, BH_3/THF 11 ml, PVA 0.5 g, PEGME 8 g). Firstly, PVA was dissolved in DMSO, and then PEGME was admixed. Secondly, the solution was stirred under nitrogen for 1 h at a temperature around 50°C. Finally BH_3/THF was added slowly to the prepared mixed solution while increasing the temperature from 50 to 100°C and then continually stirring for 24 h under nitrogen atmosphere. The synthesized PVA1PEGME and PVA2PEGME were precipitated by using diethylether and washed at least three

times in excess diethylether to remove unreacted PEGME. Then polymer gels were dried in a vacuum oven at 80°C for several days to remove residual solvent. The synthesis and the handling of the polymers was made under protective nitrogen atmosphere and finally the highly transparent, light yellow and sticky polymer was obtained and stored in a glove box (moisture content below 1 ppm). The details of the synthesis of the samples are tabulated (please see Supplementary Table).

2.3. Electrolyte preparation

All the electrolytes were prepared in the nitrogen filled glove box. For this purpose, the prepared esters were dissolved in a minimum volume of DMSO and lithium trifluoromethanesulfonate ($\text{CF}_3\text{SO}_3\text{Li}$, 97%) was added to weighed amounts of the different polymers to obtain electrolytes with the desired salt concentrations. Weighed amounts of polymer and salts were adjusted for the different levels of salt concentration corresponding to the ratios [EO]:[Li] = 10, 25, 50, 75 and 100. The resulting homogeneous viscous solution was poured on a teflon plate to get thin films. In order to ensure the complete removal of DMSO, the films were kept under high vacuum at 100°C several days.

2.4. Characterizations

^1H NMR measurements were performed with Bruker Avance 400 MHz in d-DMSO. ^{11}B NMR measurement was also made in d-DMSO using $\text{BF}_3\text{-O}(\text{C}_2\text{H}_5)_2$ as an external reference.

Prior to FT-IR spectra measurements, samples were dried under vacuum and stored in a glove box. The IR spectra ($4000\text{--}400 \text{ cm}^{-1}$, resolution 4 cm^{-1}) were recorded with a Bruker Alpha-P in ATR system.

Thermal stabilities of the polymer electrolytes were examined by thermogravimetry analysis (TGA) with a Perkin Elmer Pyris 1. The samples ($\sim 10 \text{ mg}$) were heated from room temperature to 700°C under N_2 atmosphere at a heating rate of $10^\circ\text{C min}^{-1}$.

Differential scanning calorimetry (DSC) data were recorded using a Perkin Elmer Pyris 1 instrument at a rate of $10^\circ\text{C min}^{-1}$ under a nitrogen flow.

The alternating current (AC) conductivities of the copolymer samples were measured using a Novocontrol dielectric-impedance analyzer in the frequency range from 0.1 Hz to 3 MHz as a function of temperature. The samples with a diameter of 10 mm and a thickness of approximately 0.5 mm were sandwiched between two gold-coated electrodes and their conductivities were measured at 10 K intervals under a dry nitrogen atmosphere.

Cyclic voltammograms were obtained with a potentiostat CHI instrument Model 842B. Voltammograms of PVA2PEGME550-25 were recorded in a three electrode CV system, using a polymer electrolyte modified Pt working electrode, a Li counter electrode and silver/silver chloride as reference electrode. Cyclic voltammetry studies were carried out in 0.1 M tetraethylammonium tetrafluoroborate (TBATFB)/acetonitrile.

3. Result and discussion

3.1. NMR studies

^1H NMR spectrum of the synthesized boron containing comb-branched polymer is shown in Fig. 2a. The chemical shift at 1–2 ppm (2) were attributed to the hydrogens of the CH_2 groups of PVA backbone. The methoxy groups of PEGME were observed near 3 ppm (d). The peaks between 3.20 and 3.70 ppm (c, 1) belong to ethylene oxide protons of PEG and backbone of PVA chains. The ethylene oxide protons which are linked to the boronate center appeared at 4.20 and 4.60 ppm (b, a).

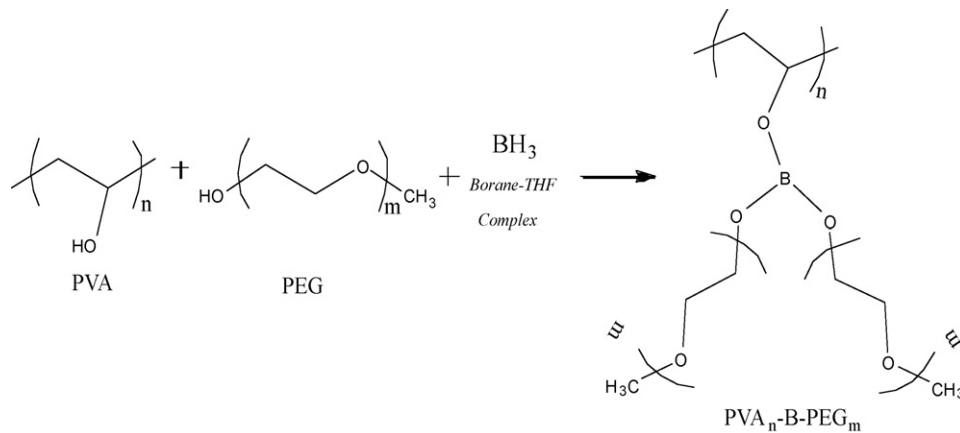


Fig. 1. Preparation and structure of PVAPEGX-Y ester copolymers.

Fig. 2b shows ^{11}B NMR spectrum of PVA2PEGME550 ester copolymer. In a previous work, it was reported that four coordinated boron sites (ring C-BO_3) usually appear close to -15 ppm and three coordinated boron sites (ring C-BO_2) appear at higher chemical shifts [30]. The shift differences due to major structural features, like the coordination of the boron sites [31]. ^{11}B NMR spec-

trum demonstrated that the resonance covering the chemical shift at -15 ppm is four coordinated and from -5 to 5 ppm is due to three coordinated boron site. The results demonstrated that the grafting occur predominantly via three coordination.

3.2. FT-IR study

Fig. 3 shows the FT-IR spectra PEGME (Fig. 3a), the copolymer PVA2PEGME550 (Fig. 3b) and the polymer electrolytes PVA2PEGME550-Y (Fig. 3c–g) with different doping ratios. All spectra contain a peak at 3400 cm^{-1} which corresponds to the absorption by hydroxyl units [32]. They also show strong bands at $2960\text{--}2800\text{ cm}^{-1}$ due to C–H stretching [33]. Characteristic main chain absorptions of the pure PVA are located at 3300 , 2934 , and 1100 cm^{-1} , corresponding to $\nu\text{O-H}$, $\nu\text{C-H}$, and $\nu\text{-C-C-O-}$, respectively. The peak at 1145 cm^{-1} (C–O, $\nu=1090\text{--}1150\text{ cm}^{-1}$) can be attributed to C–O stretching [34].

In all spectra (except PEGME), an absorption peak appeared at 662 cm^{-1} after reaction and was attributed to B–O units [31,34]. The absorption bands at ~ 1040 and ~ 1331 were assigned to the vibration of the B–O–C bond and to the anti-symmetric stretching vibration B–O, respectively [35]. The broad and intense peak of C–OH in PVA is significantly decreased in branched copolymer due to esterification reaction (Fig. 3b–g). Doping of the PVA2PEGME550

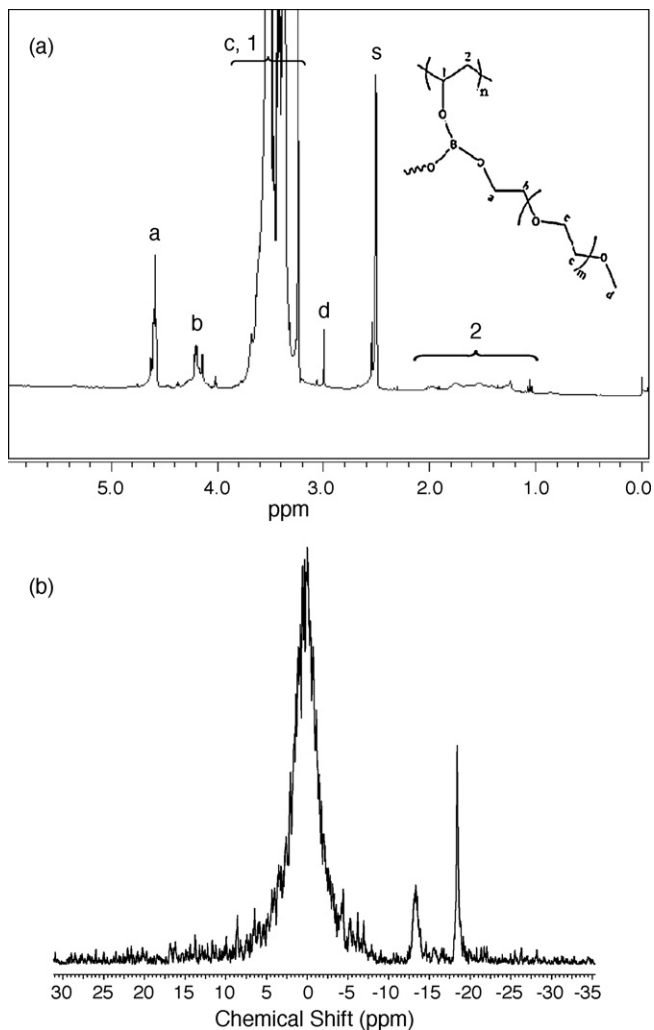


Fig. 2. (a) ^1H NMR spectra of PVA2PEGME550 ester copolymer; (b) ^{11}B NMR spectra of PVA2PEGME550 ester copolymer.

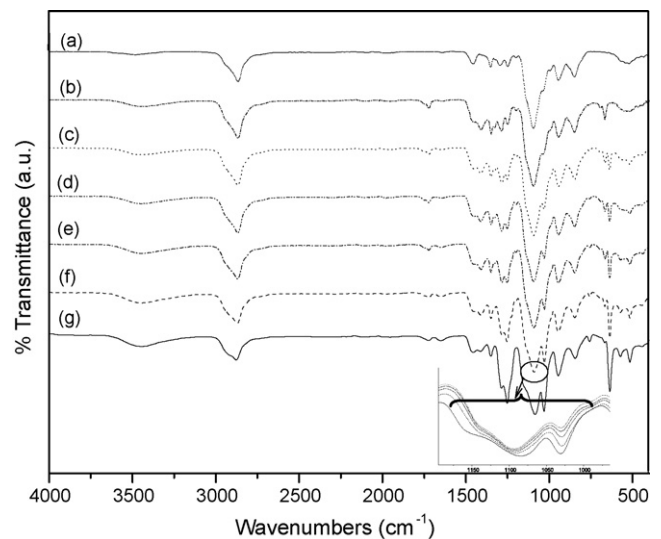


Fig. 3. Comparison of FT-IR spectra of (a) PEGME550; (b) PVA2PEGME550 and PVA2PEGME550-Y with $Y=10$ (c), 25 (d), 50 (e), 75 (f) and 100 (g).

Table 1 ΔH , T_m , eV, σ_o and T_0 values of the polymer electrolyte PVAPEGME X - Y .

	ΔH (J g ⁻¹)	T_m (°C)	eV	σ_o (S cm ⁻¹)	T_0 (°C)
PVA1PEGME350-10			0.088	0.311	-73
PVA1PEGME350-25			0.096	0.413	-87
PVA1PEGME350-100			0.170	1.655	-146
PVA1PEGME550	56.9896	12			
PVA1PEGME550-10	-	-	0.108	0.555	-95
PVA1PEGME550-50	47.7952	11			
PVA1PEGME550-75	64.9652	12.90			
PVA1PEGME750-10			0.166	0.005	-14
PVA1PEGME750-75			0.073	0.036	-86
PVA1PEGME750-100			0.050	0.005	-68
PVA2PEGME350-100			0.164	0.103	-175
PVA2PEGME550	93.2224	11.50			
PVA2PEGME550-10	-	-	0.090	0.470	-101
PVA2PEGME550-25	20.9371	6.5	0.247	97.7	-183
PVA2PEGME550-50	45.8596	9.20			
PVA2PEGME550-75	59.2853	11.70	0.104	0.53	-122
PVA2PEGME550-100			0.069	0.092	-80
PVA2PEGME750	76.3780	22.70			
PVA2PEGME750-25	36.5320	12.30			
PVA2PEGME750-50	64.6767	19			
PVA2PEGME750-75	76.1941	22.70			

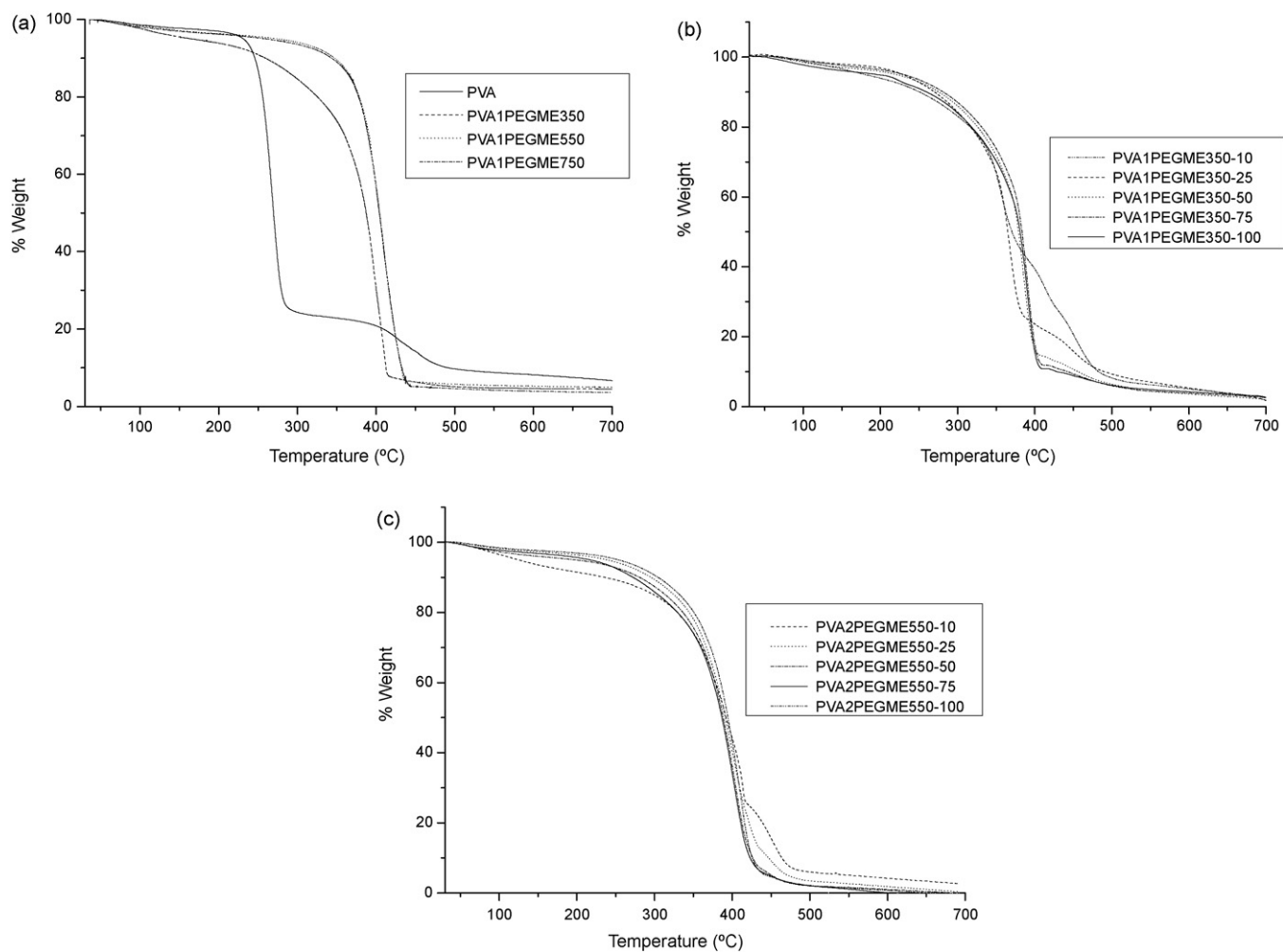


Fig. 4. (a) TGA curves of PVA and PVA1PEGME X with $X=350, 550$ and 750 . The heating rate was $10^\circ\text{C min}^{-1}$. (b) Comparison of the weight loss of polymer electrolytes PVA1PEGME350- Y with $Y=10, 25, 50, 75$ and 100 . The heating rate was $10^\circ\text{C min}^{-1}$. (c) Comparison of the weight loss of polymer electrolytes PVA2PEGME550- Y with $Y=10, 25, 50, 75$ and 100 . The heating rate was $10^\circ\text{C min}^{-1}$.

electrolyte with $\text{CF}_3\text{SO}_3\text{Li}$ with different ratios will create two phenomena:

- (1) Significant changes occurred only in the region of the peak attributed to the C–O–C group. Indeed, for electrolytes containing $\text{CF}_3\text{SO}_3\text{Li}$, this peak was slightly broadened, indicating a higher degree of interactions by co-ordination between Li^+ and EO [36].
- (2) As it can be seen from Fig. 3(b–g), after doping with $\text{CF}_3\text{SO}_3\text{Li}$ new peak was formed at 639 cm^{-1} which belongs to $\text{CF}_3\text{SO}_3\text{Li}$.

3.3. Thermal properties

The thermal stability is an important property for electrolytes composed of polymers and lithium salts during application in lithium-ion polymer batteries. The thermal stability was evaluated by TGA for the neat polymer and the electrolytes with various Li-salt. Fig. 4a shows TG thermogram of the pure PVA and the neat polymers PVA1PEGME350, PVA1PEGME550 and PVA1PEGME750. As seen, the onset of degradation temperature of PVA is approximately $225\text{ }^\circ\text{C}$. For all the neat polymers, two steps of weight losses were noticed within the temperature range of

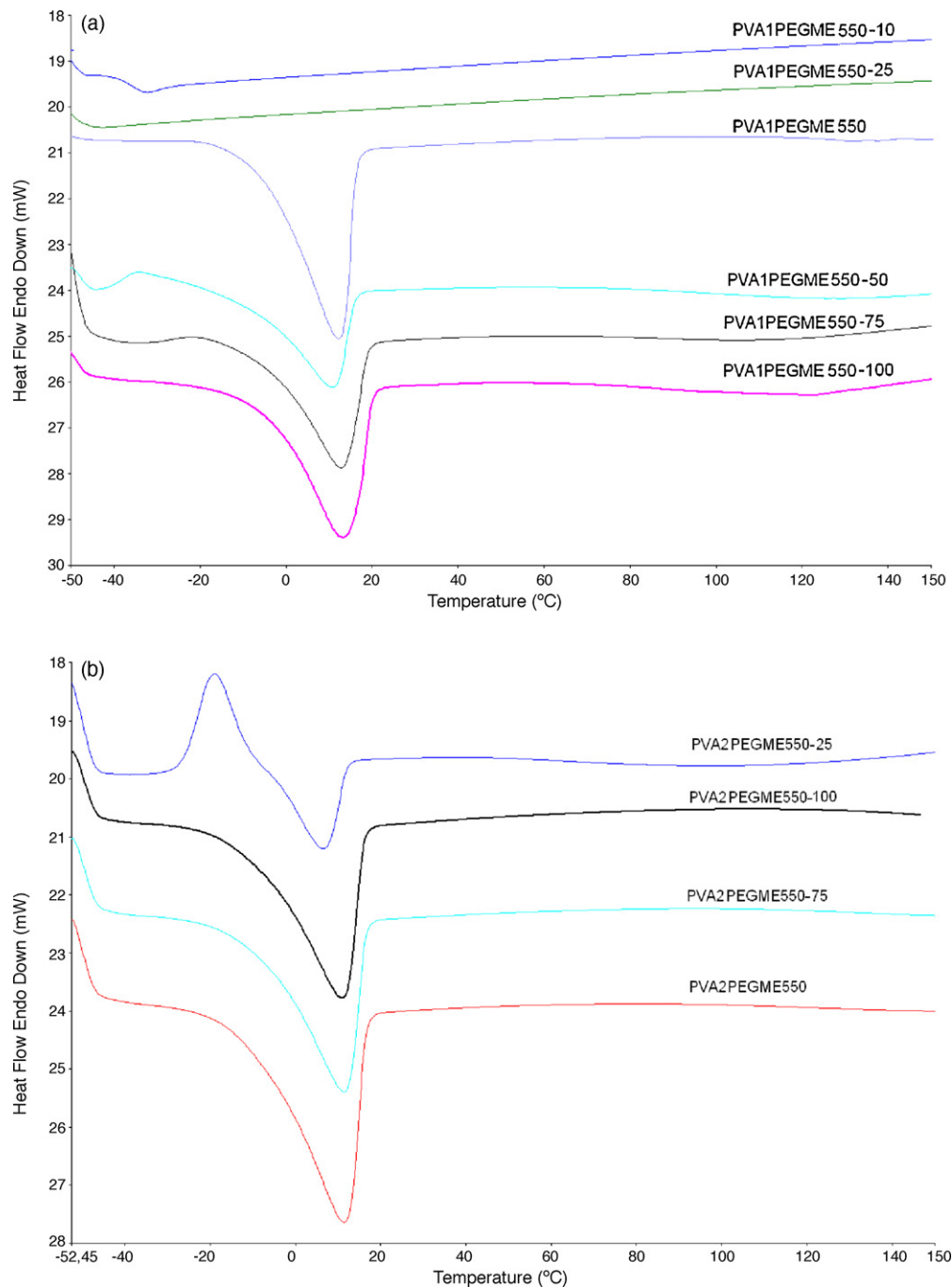


Fig. 5. (a) DSC thermograms of PVA1PEGME550 and the polymer electrolytes PVA1PEGME550-Y with $Y = 10, 25, 50, 75$ and 100 . Second heating run endotherms are presented at a heating rate of $10\text{ }^\circ\text{C min}^{-1}$; (b) DSC thermograms of polymer PVA2PEGME550 and the polymer electrolytes PVA2PEGME550-Y with $Y = 25, 75$ and 100 . Second heating run endotherms are presented at a heating rate of $10\text{ }^\circ\text{C min}^{-1}$; (c) DSC thermograms of polymer PVA2PEGME750 and the polymer electrolytes PVA2PEGME750-Y with $Y = 25, 50, 75$ and 100 . Second heating run endotherms are presented at a heating rate of $10\text{ }^\circ\text{C min}^{-1}$.

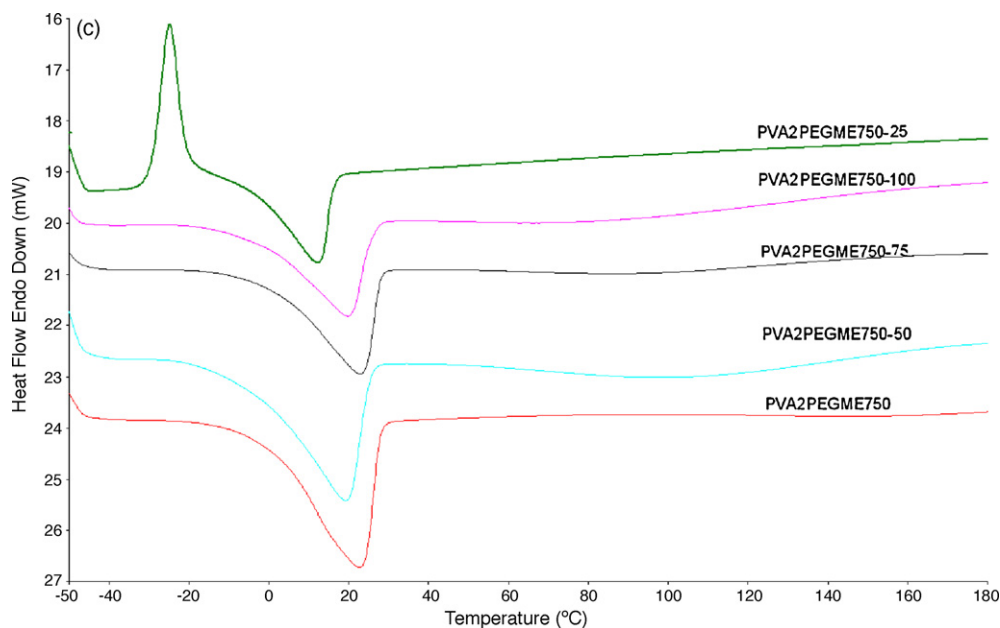


Fig. 5. (Continued).

measurement. The first step elusive weight change up to 200 °C represents us that, on one hand, the evaporation of remained solvent (DMSO) which may not be removed during drying process. On the other hand, it may be due to the loss of low molecular weight compounds produced through molecular rearrangements of the polymer. The second step of the weight loss which starts above 350 is due to degradation of the materials. The decomposition temperature of PVA1PEGME350 is approximately 300 °C whereas it was found to be approximately 350 °C for PVA1PEGME550 and PVA1PEGME750. The thermal stability was investigated for all neat polymers after the PEGME grafted to PVA. Fig. 4b and c shows the TGA traces of the polymer electrolytes PVA1PEGME350-Y and PVA2PEGME550-Y, and it was observed that the electrolytes are thermally stable up to nearly 250 and 300 °C, respectively.

The thermal properties of the neat polymer and the electrolytes with various Li-salt were investigated using DSC as well. ΔH_m is the heat of fusion for the electrolytes which can be calculated from the integral area of the baseline and of each melting curve. The baseline can be designated by connecting two points at which the instant value of its derivative curve becomes zero near melting temperature (T_m) [18]. The data of ΔH_m and T_m , evaluated during the heating process from -50 to 150 °C, are all summarized in Table 1.

Fig. 5(a–c) shows the melt endotherms of semi-crystalline PEGME of comb-branched copolymer and the doped samples. The electrolytes PVA1PEGME550-10 and PVA1PEGME550-25 were fully amorphous, while the PVA1PEGME550 polymer and electrolytes of PVA1PEGME550-50, PVA1PEGME550-75 and PVA1PEGME550-100 displayed melting transitions at 12, 11, 12.90 and 13.20 °C, respectively (Fig. 5a). The PVA2PEGME550 polymer and electrolytes of PVA2PEGME550-25, PVA2PEGME550-75, PVA2PEGME550-100 showed melting transitions at 11.50, 6.5, 11.70, 11 °C, respectively. Cold crystallizations were observed at -20 and -25 °C for the electrolytes of PVA2PEGME550-25 and PVA2PEGME750-25 before the melting peak (Fig. 5b and c). Furthermore, PVA2PEGME750 polymer and electrolytes of PVA2PEGME750-25, PVA2PEGME750-50, PVA2PEGME750-75, PVA2PEGME750-100 displayed melting transitions at 22.70, 12.30, 19.05, 22.75 and 19.75 °C, respectively.

3.4. Ionic conductivity

The ionic conductivity of lithium ion in polymer electrolytes containing PVAPEGMEX-Y with different M_w of PVA and changing PEGME pendant side units was measured by the ac impedance technique. The polymer electrolyte films were cut into disks of 10 mm in diameter sandwiched between Pt electrodes and subjected to the impedance analyzer in a completely water-free environment. In order to understand the ion dynamics in the polymer electrolytes, the frequency dependence of the conductivity at various temperatures has been analyzed for all samples. Fig. 6 shows the frequency dependence of the ac conductivity (σ_{ac}) at various temperatures for PVA2PEGME550-25.

The frequency-dependent ac conductivity curves show a general trend for all samples and at all temperatures in the log–log plot of Fig. 6. As can be distinguished clearly from Fig. 6, the curves of ac conductivity versus frequency for various temperatures exhibits almost linear increasing at low frequencies which is assigned to the

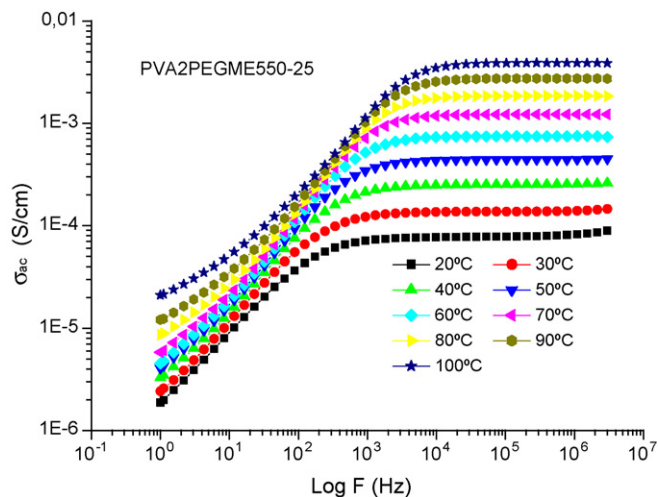


Fig. 6. The frequency dependent ac conductivity of anhydrous PVA2PEGME550-25 at various temperatures.

polarization of the blocking Pt electrodes, while well-developed frequency independent plateaus are observed at higher frequencies.

The switchover from the frequency independent to frequency dependent region marks the onset of conductivity relaxation that gradually shifts to higher frequencies as temperature increases Fig. 6. The frequency independent conductivity is, in general, identified with the dc conductivity (σ_{dc}). The dc conductivities were obtained by linear fitting of the frequency independent region of the σ_{ac} . A similar kind of frequency dispersion was observed for all other compositions as well.

The obtained σ_{dc} variation of the PVAPEGME-X-Y as a function of temperature are shown in Fig. 7(a–b), where conductivity has been plotted as a function of $1000/T$. It can be seen from the plots that the temperature dependence of conductivity deviates from the Arrhenius behavior. The curved lines indicate that the ion conduction in these polymer electrolytes can be explained by the concept of free volume [37,38], which is expressed by the Vogel–Tamman–Fulcher (VTF) (Eq. (1)). To have better insight into the temperature dependence of σ_{dc} , the conductivity data have been fitted to the equation.

$$\sigma = \sigma_0 \exp \frac{-B}{k(T - T_0)} \quad (1)$$

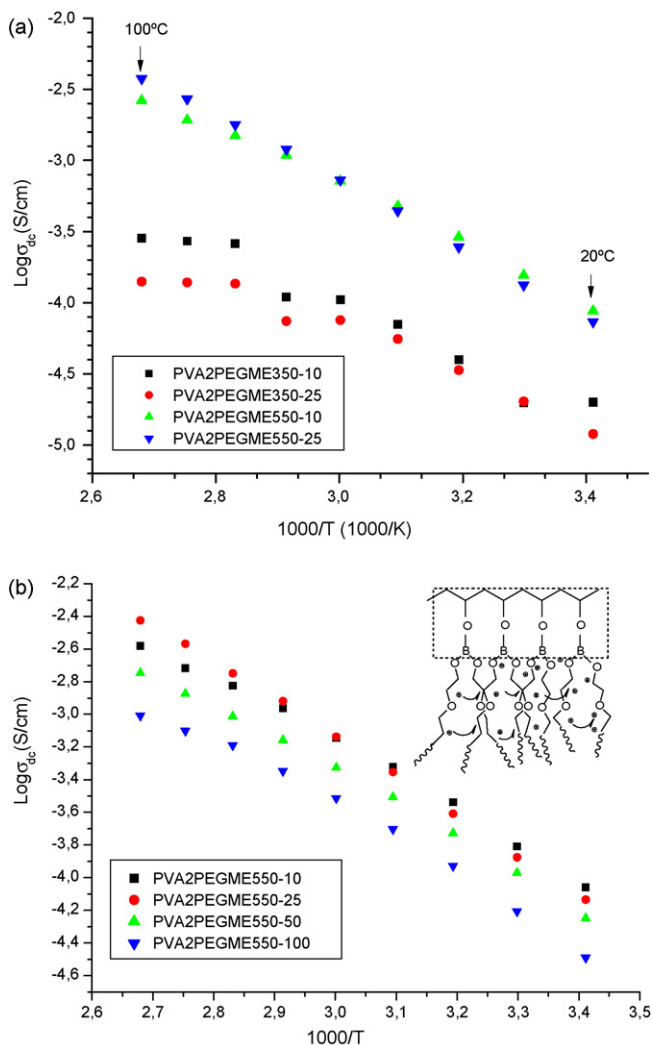


Fig. 7. Temperature dependence of the DC conductivities of PVA2PEGME350-Y and PVA2PEGME550-Y based materials with Y = 10, 25; (b) temperature dependence of the DC conductivities of PVA2PEGME550-Y based materials.

where σ_0 is the prefactor, T is the absolute temperature, k is the Boltzmann constant, B is an apparent activation energy and T_0 is the equilibrium glass transition temperature at which the “free” volume disappears or at which configuration free entropy becomes zero (i.e., molecular motions cease). The VTF parameters of the samples are given in Table 1.

The polymer electrolytes have comb-like copolymer structure as PEGME being side chain, and as a result the copolymer has a special structure which can lead to the lithium ion conductivity. A comparison between the conductivities of the electrolytes with different chain lengths is shown in Fig. 7a. It indicates that at a given temperature the conductivities of the polymer electrolytes increases with length of PEGME incorporated in the polymer main chain, which acts as a plasticizer mainly to the matrix polymer [39]. It is generally considered in polymer electrolytes that ionic conduction occurs by segmental motion of polymer chains in amorphous region [40–42]. T_g is correlated with flexibility of EO chains, i.e., T_g is correlated with segmental motion of EO chains. Accordingly, mobility of carrier ions in polymer electrolytes is correlated with T_g [43–45]. The temperature range for the ionic conductivities of the present study shown in Fig. 7(a–b) is above T_g 's. In other words, the ionic conductivities of polymer electrolytes whose phase is almost amorphous were measured in the present study. In Fig. 7a the deviations in PVA2PEGME350-10 and PVA2PEGME350-25 from VTF $1000/T \sim 2.8$ – 2.9 can be expressed by the melting transition.

Fig. 7b shows the variation of conductivity at different temperatures as a function of EO/Li ratio. The conductivity increased gradually with increasing salt concentration and reached a maximum for EO/Li = 25 (i.e., $1.8 \times 10^{-3} \text{ S cm}^{-1}$ at 80°C , and $3.9 \times 10^{-3} \text{ S cm}^{-1}$ at 100°C). Conductivity decreased with further addition of salt. This tendency of salt containing PEO electrolytes has previously been attributed to the formation of ionic clusters, reducing the number and the overall mobility of the ions [46]. A further reason for the high conductivities of the electrolytes having low salt concentrations is the relatively low level of ion–polymer interaction. Indeed, it has been proposed that one Li^+ is coordinated by four ethylene oxide oxygens in PEO, leading to “transient cross-links” which reduce the segmental mobility of the polymer [47]. The electrolytes having low salt concentrations thus had relatively low T_g 's, as explained by DSC results. In addition, the solvating effects of different segment sizes may also play a significant role in the ionic conductivity.

Kato et al. [48] showed that the high degree of dissociation of $\text{CF}_3\text{SO}_3\text{Li}$ might be induced by the Lewis acidic PEG–borate ester. In other words, the PEG–borate ester with Lewis acidity interacts with the anions, leading to improved dissociation of Li–salts and transport number of lithium ions. Therefore the interaction between the PEG–borate ester and the CF_3SO_3^- should be higher which can be related to order of “hardness” of the Lewis basic anions, $\text{CF}_3\text{SO}_3^- > \text{ClO}_4^- > \text{N}(\text{CF}_3\text{SO}_2)_2^-$, estimated by ab initio calculations [49]. As a consequence, the PEG–borate ester in polymer electrolytes improves ionic conductivity as a plasticizer and Lewis acid. Additionally, Lewis acidity of the PEG–borate ester is particularly effective for enhancement of the degree of Li-salt dissociation on $\text{CF}_3\text{SO}_3\text{Li}$ [48]. PEG–boronate ester polymers was studied by Jannasch for electrochromics and it was generally found that, at a given temperature and salt concentration, the conductivity of the electrolytes increased with the length of the side chain segment [33]. Poly(vinyl borate), PVBO and lithium derivative of PVBO, which was prepared by homogeneous esterification of PVA with boric acid, was studied in the literature. It was showed that there is more than hundred time increase of conductivity in the case of PVBO–Li and so it behaves as moderately good polyelectrolyte and become comparable with the literature [34].

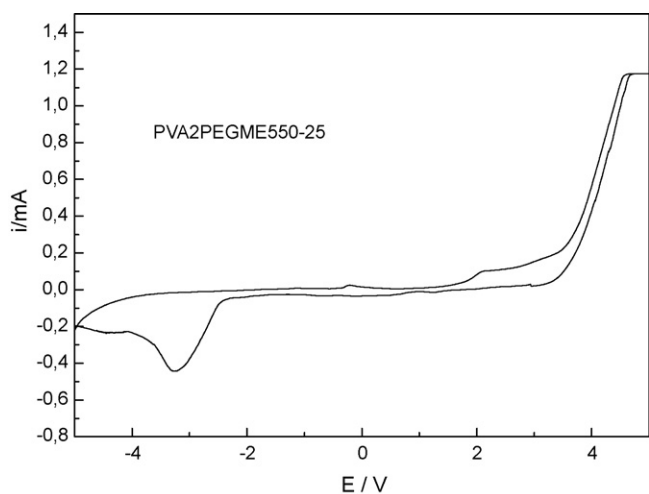


Fig. 8. Cyclic voltammogram of PVA2PEGME550-25 using platinum working electrode and lithium counter electrode.

3.5. Electrochemical stability

The electrochemical stability of the any device, particularly energy storage devices, provides essential information for assessing the success. Cyclic voltammetry was performed at room temperature and demonstrated in Fig. 8. The salt-doped grafted polymer PVA2PEGME550-25 showed an excellent electrochemical stability window of approximately 4V. A slight rise at ~4V can be associated with the breakdown of the lithium salt and related to the anion oxidation followed by a possible polymeric degradation [50]. The wide cathodic peak between -2.5 and -3.5V was attributed to salt reduction.

4. Conclusions

In the present work, a novel comb-branched boron containing copolymers with different molecular weight PEGME sides were produced. Then polymer electrolytes were synthesized after doping the host material with lithium salt at several molar ratios, i.e., EO/Li. The branched EO units of the copolymer are capable of forming donor-acceptor type bonds by complexing with the metal ion. These polymer electrolytes were characterized using DSC, FT-IR, ^1H NMR and dielectric-impedance spectroscopy. ^{11}B NMR result demonstrated three coordinated boron site. The conductivity studies illustrate that the ionic conductivity of these polymer electrolytes was found to be dependent on side chain length as well as the Li^+ content. The polymer electrolyte PVA2PEGME550-25 illustrated a satisfactory ionic conductivity of $8.9 \times 10^{-5} \text{ S cm}^{-1}$ at 20°C and $3.9 \times 10^{-3} \text{ S cm}^{-1}$ at 100°C . The polymer electrolytes with higher Li^+ content shows VTF behavior, indicating that the Li^+ ion motion is depended on the flexibility of the polymer side chain. These materials have high ion conductivity and can be suggested for application to lithium ion batteries.

Acknowledgement

This work was supported by BOREN under Contract number 2009.Ç0213.

Appendix A. Supplementary data

Supplementary data associated with this article can be found, in the online version, at doi:10.1016/j.jpowsour.2010.08.020.

References

- [1] W.H. Meyer, *Mater. Adv.* 10 (6) (1998) 439–448.
- [2] B. Scrosati, *Chem. Rec.* 5 (5) (2005) 286.
- [3] C.A. Vincent, B. Scrosati, *Bull. Mater. Res. Soc.* 25 (2000) 28.
- [4] J.M. Tarascon, M. Armand, *Nature* 414 (2001) 359.
- [5] J. Sun, D.R. MacFarlane, *Electrochim. Acta* 40 (13–14) (1995) 2301.
- [6] D.R. MacFarlane, J. Sun, M. Forsyth, J.M. Bell, L.A. Evans, I.L. Skyrabin, *Solid State Ionics* 86–88 (1996) 959.
- [7] K.M. Abraham, *Electrochim. Acta* 38 (1993) 1233.
- [8] P.G. Bruce, *Electrochim. Acta* 40 (1995) 2077.
- [9] Z. Gadajourova, Y.G. Andreev, D.P. Tunstall, P.G. Bruce, *Nature* 412 (2001) 520.
- [10] P. Lightfoot, M.A. Metha, P.G. Bruce, *Science* 262 (1993) 883.
- [11] F. Croce, R. Curini, A. Martinelli, L. Persi, F. Ronci, B. Scrosati, *J. Phys. Chem. B* 103 (1999) 10632.
- [12] D.E. Fenton, J.M. Parker, P.V. Wright, *Polymer* 14 (1973) 589.
- [13] M.B. Armand, S.M. Chabagno, M. Duclot, Second International Meeting on Solid Electrolytes, St. Andrews, Scotland Extended Abstracts, 20–22 September, 1978.
- [14] Y.K. Yarovoy, H.P. Wang, S.L. Wunder, *Solid State Ionics* 118 (1999) 301.
- [15] H.P. Wang, H. Huang, S.L. Wunder, *J. Electrochem. Soc.* 147 (2000) 2853.
- [16] K. Murata, S. Izuchi, Y. Yoshihisa, *Electrochim. Acta* 45 (2000) 1501.
- [17] Y.J. Shen, M.J. Reddy, P.P. Chu, *Solid State Ionics* 175 (2004) 747–750.
- [18] Q. Xiao, X. Wang, W. Li, Z. Li, T. Zhang, H. Zhang, *J. Membr. Sci.* 334 (2009) 117–122.
- [19] D.J. Lin, C.L. Chang, C.K. Lee, L.P. Cheng, *Eur. Polym. J.* 42 (2006) 2407–2418.
- [20] M. Wang, L. Qi, F. Zhao, S. Dong, *J. Power Sources* 139 (2005) 223–229.
- [21] P.G. Hall, G.R. Davis, J.E. McIntyre, I.M. Ward, D.J. Banister, K.M.F. Le Brocq, *Polym. Commun.* 27 (1986) 98.
- [22] D. Fish, I.M. Khan, J. Smid, *Macromol. Chem. Rapid Commun.* 7 (1986) 115.
- [23] R. Spindler, D.F. Shriver, *J. Am. Chem. Soc.* 10 (1988) 3036.
- [24] E.F. Reis, F.S. Campos, A.P. Lage, R.C. Leite, et al., *Mater. Res.* 9 (2006) 185.
- [25] N.A. Peppas, N.K. Mongia, *Eur. J. Pharm. Biopharm.* 43 (1997) 52.
- [26] S. Hashimoto, K. Furukawa, *Biotechnol. Bioeng.* 30 (1987) 52.
- [27] D.S. Kim, T.I. Yun, M.Y. Seo, H.I. Cho, et al., *Desalination* 200 (2006) 634.
- [28] A. Martinelli, A. Matic, P. Jacobsson, L. Börjesson, M.A. Navarra, A. Farnicola, S. Panero, B. Scrosati, *Solid State Ionics* 117 (2006) 2431.
- [29] Y. Miyazaki, K. Yoshimura, Y. Miura, H. Sakashita, K. Ishimura, *Polyhedron* 22 (2003) 909–916.
- [30] A. Sezgin, Ü. Akbey, M.R. Hansen, R. Graf, A. Bozkurt, A. Baykal, *Polymer* 49 (18) (2008) 3859–3864.
- [31] P.-Y. Pennarun, P. Jannasch, *Solid State Ionics* 176 (2005) 1103–1112.
- [32] P. Chetri, N.N. Dass, N.S. Sarma, *Mater. Sci. Eng. B* 139 (2007) 261–264.
- [33] M. Şenel, A. Bozkurt, A. Baykal, *Ionics* 13 (2007) 263–266.
- [34] P.-Y. Pennarun, P. Jannasch, S. Papaefthimiou, N. Skarpentzos, P. Yianoulis, *Thin Solid Films* 514 (2006) 258–266.
- [35] P.-Y. Pennarun, P. Jannasch, *Solid State Ionics* 176 (2005) 1849–1859.
- [36] M.H. Cohen, D. Turnbull, *J. Chem. Phys.* 31 (1959) 1164.
- [37] G.S. Grest, M.H. Cohen, *Phys. Rev. B* 21 (1980) 4113.
- [38] Y. Kato, K. Hasumi, S. Yokoyama, T. Yabe, H. Ikuta, Y. Uchimoto, M. Wakihara, *Solid State Ionics* 150 (2002) 355.
- [39] D.F. Shriver, G.C. Farrington, *C&E News* 20 (1985) 42.
- [40] S. Harris, D.F. Shriver, M.A. Ratner, *Macromolecules* 19 (1986) 987.
- [41] A.L. Tipton, M.C. Lonergan, M.A. Ratner, D.F. Shriver, T.T.Y. Wong, K. Han, *J. Phys. Chem.* 98 (1994) 4148.
- [42] B.L. Papke, M.A. Ratner, D.F. Shriver, *J. Electrochem. Soc.* 129 (1982) 1694.
- [43] P.G. Bruce, C.A. Vincent, *J. Chem. Soc., Faraday Trans.* 89 (1993) 3187.
- [44] L.R.A.K. Bandara, M.A.K.L. Dissanayake, B.-E. Mellancer, *Electrochim. Acta* 43 (1998) 1475.
- [45] M. Mendolia, H. Cai, G.C. Farrington, *Application of Electroactive Polymers*, 1st ed., Chapman & Hall, London, 1993, p. 113.
- [46] R.G. Linford, *Application of Electroactive Polymers*, 1st ed., Chapman & Hall, London, 1993.
- [47] Y. Kato, S. Yokoyama, T. Yabe, H. Ikuta, Y. Uchimoto, M. Wakihara, *Electrochim. Acta* 50 (2004) 281–284.
- [48] Y. Kato, K. Suwa, H. Ikuta, Y. Uchimoto, M. Wakihara, S. Yokoyama, T. Yabe, M. Yamamoto, *J. Mater. Chem.* 13 (2003) 280.
- [49] C.P. Fonseca, D.S. Rosa, F. Gaboardi, S. Neves, *J. Power Sources* 155 (2006) 381–384.